# DEVELOPMENT OF AN ADVANCED MICROELECTRONIC CONNECTION WELDING SYSTEM

FINAL REPORT

NAS8-24490

March 1970

by

William G. Cunningham, Senior Manufacturing Engineer
Ralph R. Braswell, Electronic Design Analyst

Prepared For

George C. Marshall Space Flight Center
Marshall Space Flight Center, Alabama 35812

Martin Marietta Corporation
Advanced Manufacturing Technology Department
Orlando, Florida 32805



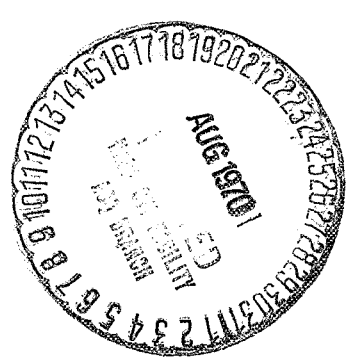


OR 10,639

# DEVELOPMENT OF AN ADVANCED MICROELECTRONIC CONNECTION WELDING SYSTEM

FINAL REPORT

NAS8-24490

March 1970

by

William G. Cunningham, Senior Manufacturing Engineer
Ralph R. Braswell, Electronic Design Analyst

Prepared For

George C. Marshall Space Flight Center
Marshall Space Flight Center, Alabama 35812

Martin Marietta Corporation
Advanced Manufacturing Technology Department
Orlando, Florida 32805

OR 10,639

ACKNOWLEDGEMENTS

This program was conducted by the Advanced Manufacturing technology personnel of the Martin Marietta Corporation's Orlando Florida Division. The authors wish to acknowledge contributions to the technical achievements of this program made by Mr. Wendell R. Hutchinson, Task Leader and Mr. Forest Deal, Senior Manufacturing Engineer. In addition, recognition is given to Messers Truit Vann and John Rasquin of the Marshall Space Flight Center for their cooperation during the performance of this program.

CONTENTS

ILLUSTRATIONS

ABSTRACT

A prototype infrared radiation (IR) feedback control system for the microweld process has been developed at the Martin Marietta Corporation, Orlando Division as a result of the work on this program. The feasibility of applying feedback control to the microwelding process has been demonstrated.

A laboratory model of the control system was breadboarded and numerous welds were made. The system demonstrated that within its control range wide fluctuations in power supply energy setting had small effects on the pull strength of welds.

The system is pictured in Figure A. The modifications necessary to the power supply are simple and can be built as a ''bolt-on'' unit at the rear of the supply.

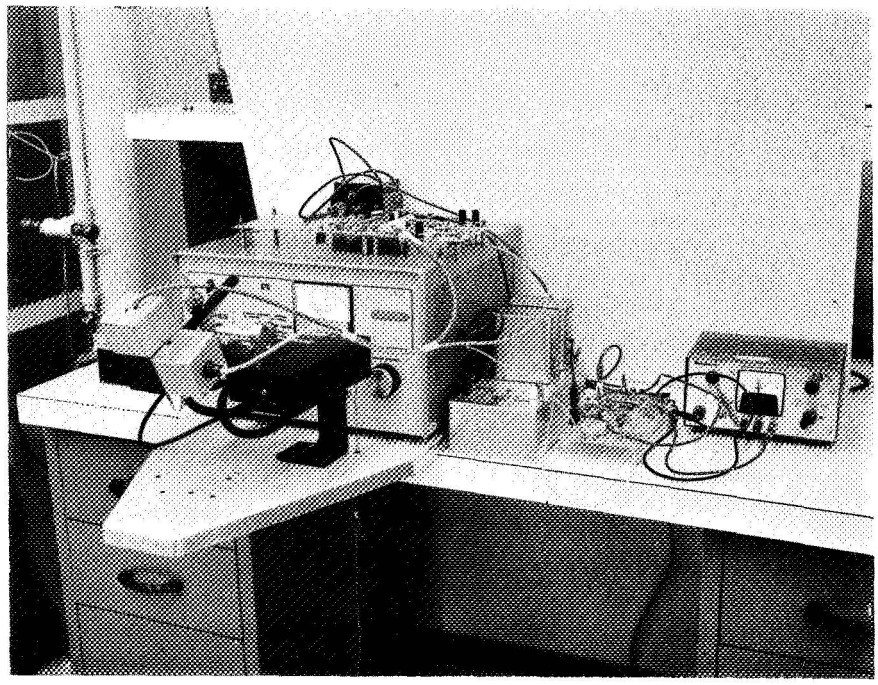

Figure A. Complete Feedback System

# I. INTRODUCTION

In today's missile systems, electronic circuits are required to withstand severe environmental exposure. In addition, these systems have to be highly reliable. Component reliability can be achieved by 100 percent testing if necessary or by selective purchasing, but component lead interconnections are another matter. In many cases the constraints imposed on these interconnections by the environment necessitate their being joined by welding, a process in which reliability is assumed by correlation and verified by destructive testing.

With the advent of quantum infrared detectors, it is possible to use nondestructive testing (NDT) techniques for in-process monitoring (Reference 1). The next logical extension of these techniques is closed loop feedback control of the weld process.

This study was designed to improve the reliability of microwelding by demonstrating the effective use of feedback controls to remove the influence of the power supply from the weld process.

## II. DEVELOPMENT

The system as developed is shown in diagram on Figure 1. The following discussion will treat the various subsystems, that make up the total system, separately.

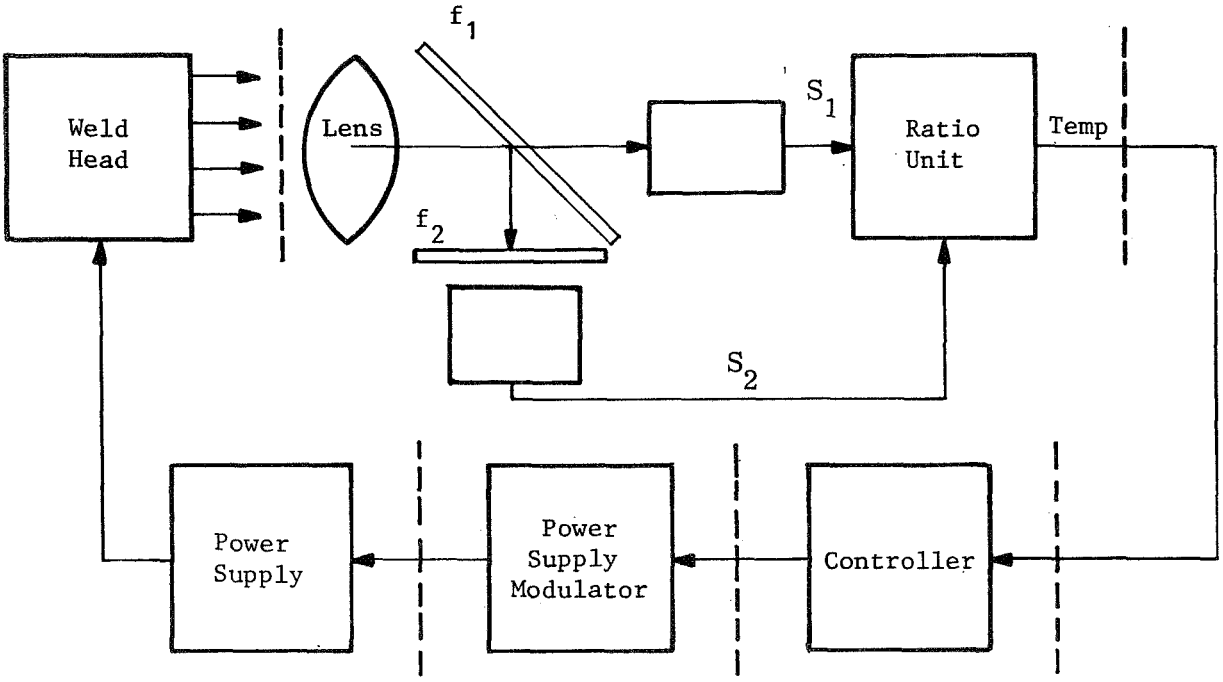


Figure 1. Block Diagram Complete System

### A. THE SENSOR SUBSYSTEM

In any closed loop operation, the quantity being measured must truly be representative of the physical process involved. In addition this measured variable must be most affected by whatever control action is taken. In any photoconductive device, the output varies proportionately to the radiant energy seen by the active element. A practical consequence of this situation is that source area variations appear as changes in temperature. Clearly this is unacceptable.

However, if two active elements were to be used, each looking at a different portion of the spectrum, then the ratio between the outputs would be insensitive to variations in source area (see Equation 6 in Appendix I). Furthermore, the actual value of this ratio is a measure of the temperature of the device under observation.

A two wavelength sensor was developed (Figure 2) along the line presented above. It has been demonstrated in the laboratory that the ratio between the detector outputs is independent of source area.

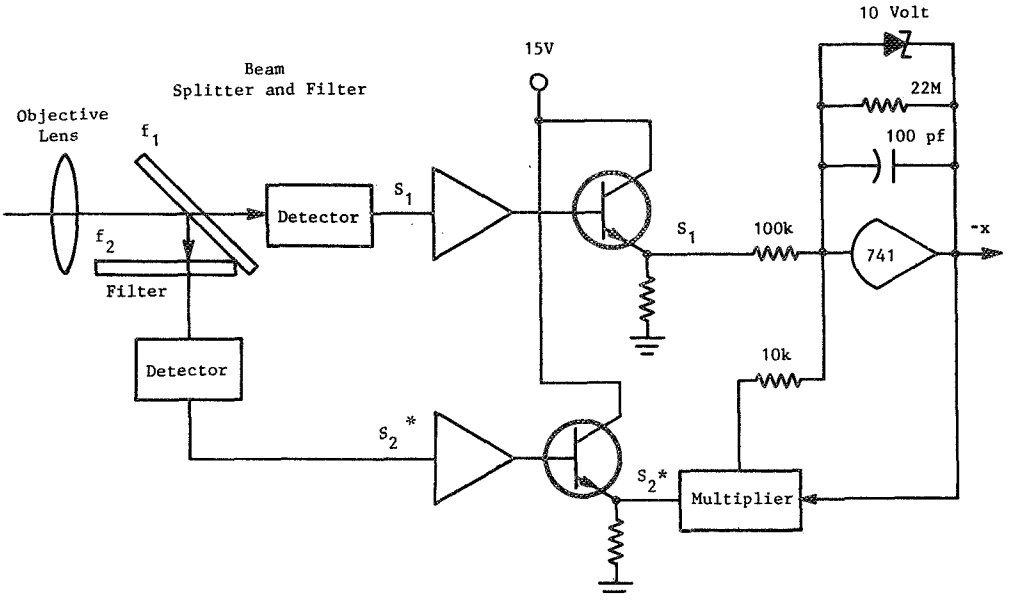


Figure 2. Sensor Subsystem

The filters incorporated into the two wavelength sensor have band passes of 2.84 to 2.97 micron and 2.02 to 2.13 micron ($10^{-4}$ cm). A typical calibration chart is presented in Figure 3. These filters are of the reflecting rather than the absorbing type, which allows the use of one of the filters as a beam splitter (see Figure 2).

Figures 4 and 5 show the two wavelength sensor subsystem mounted and viewing the weld process.

In addition to designing a sensor system one must also determine where the proper viewing point for the weld is. That is, the more IR energy that can be collected on the active elements of the detectors, the less stringent become the amplifier requirements.

A photo/optical technique was devised to fully see the radiation patterns emitted during a weld. The system that emerged is shown in Figure 6 and typical results are shown in Figure 7. The technique involved building a ''birdcage'' around the weld area. The cage was used to support IR sensitive film. The film was exposed by the energy released during a weld.

The sinusoidal pattern shown is explained by the presence of shadows produced by the cross wires being welded.

The shape of the radiation pattern dictates the sensor position. That is, the sensor should be so placed that it observes the area between two of the shadows.

Once radiation patterns were known and the optimum sensor position determined the sensor could be installed on the weld supply.

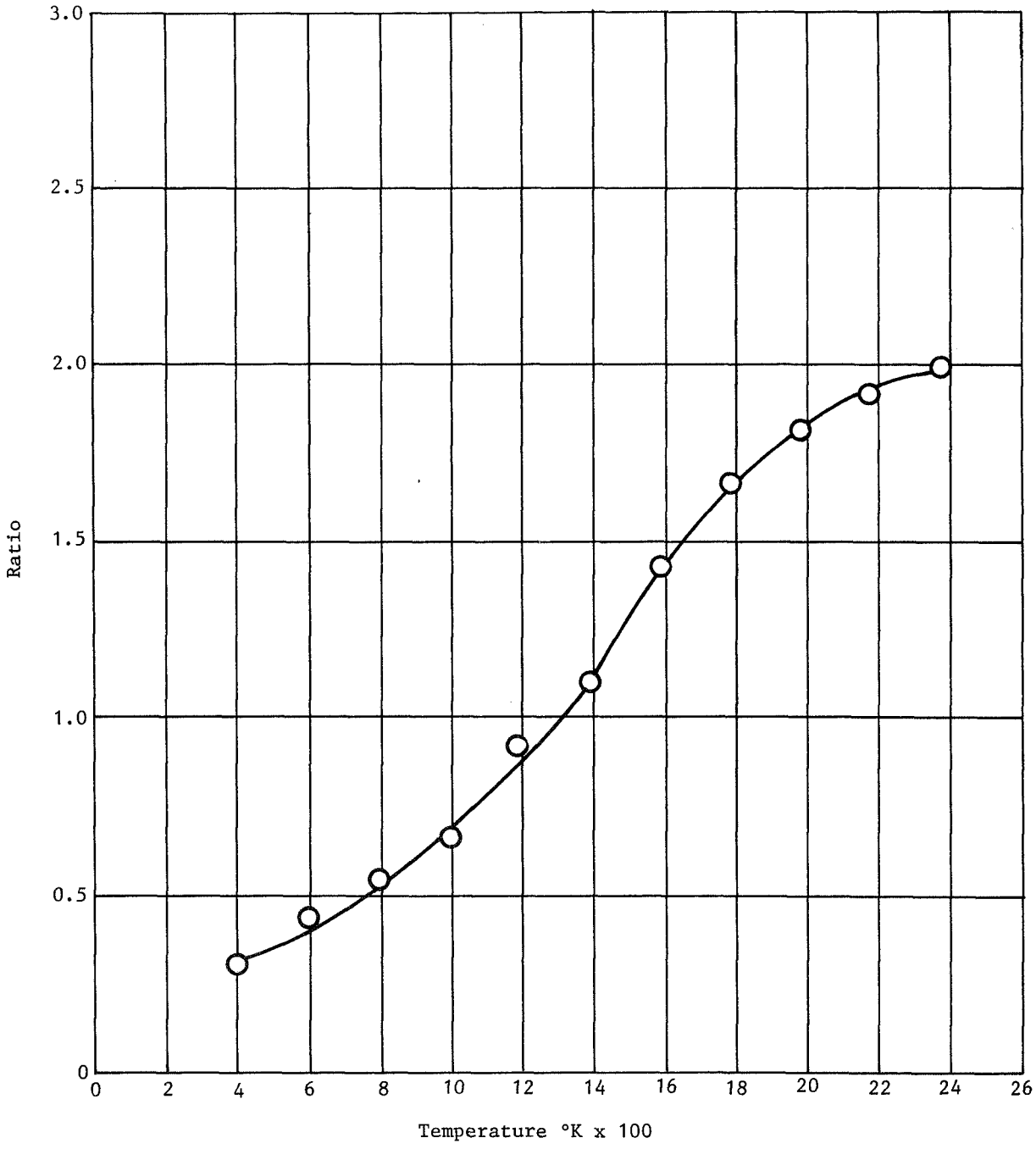


Figure 3. Typical Ratio Unit Output

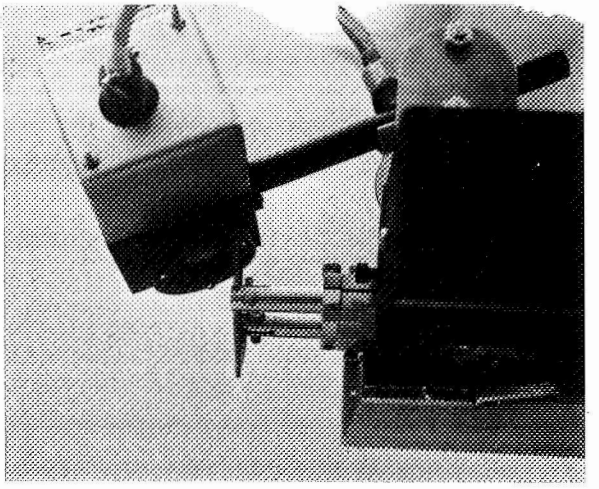

Figure 4. Two Wavelength Sensor

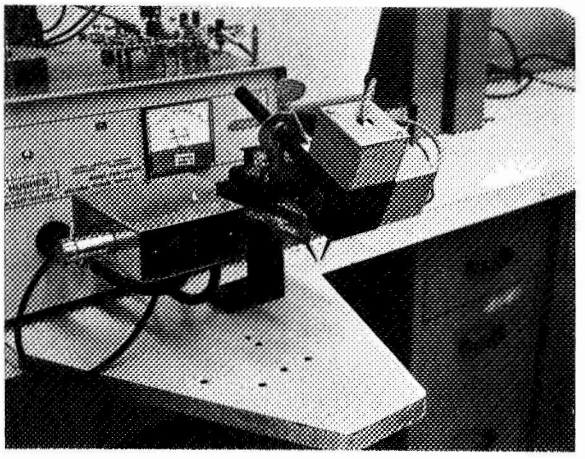

Figure 5. Overview of Two Wavelength Sensor

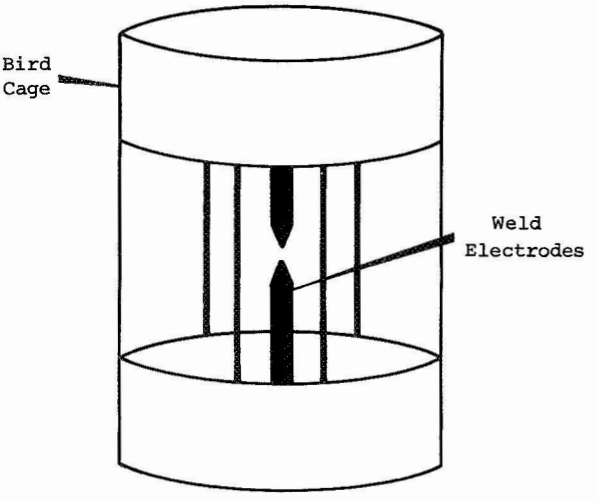


Figure 6. Photo/Optical System Diagram

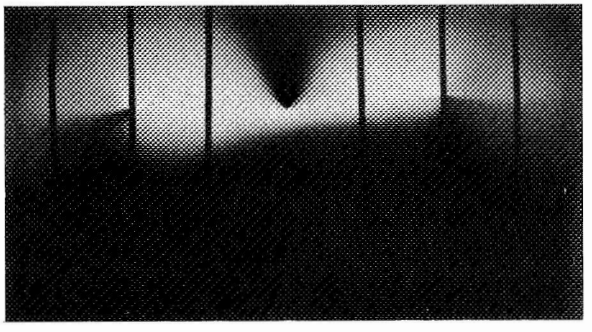

Figure 7. Sinusoidal Pattern

The sensor subsystem electronics posed quite a problem. We deal with such small signals from the detectors, that high gain amplifiers are necessary.

The above constraints require that the amplifiers be physically isolated and enclosed each in its own mu-metal shield.

This approach yielded several significant benefits:

1 Noise was reduced to a tolerable level

2 Cross-talk between sensor signals was all but eliminated.

The reader is referred to Appendix II, Part A for a detailed explanation of the circuitry in the ratio unit. It suffices at this point to restate equation 4 in Appendix II:

$$\text{Ratio} = x = -\frac{S_1^*}{S_2^*}\left[\frac{1}{\frac{\tau}{S_2^*}S+1}\right]$$

where $\tau$ = time constant = $10^{-5}$s.

The above simply states that the ratio of the two sensor outputs is equal to $S_1^*$ divided by $S_2^*$ with some filtering.

## B. CONTROL ELECTRONICS

For the purpose of demonstrating feasibility of this system a proportional controller was build and is shown in Figure 8.

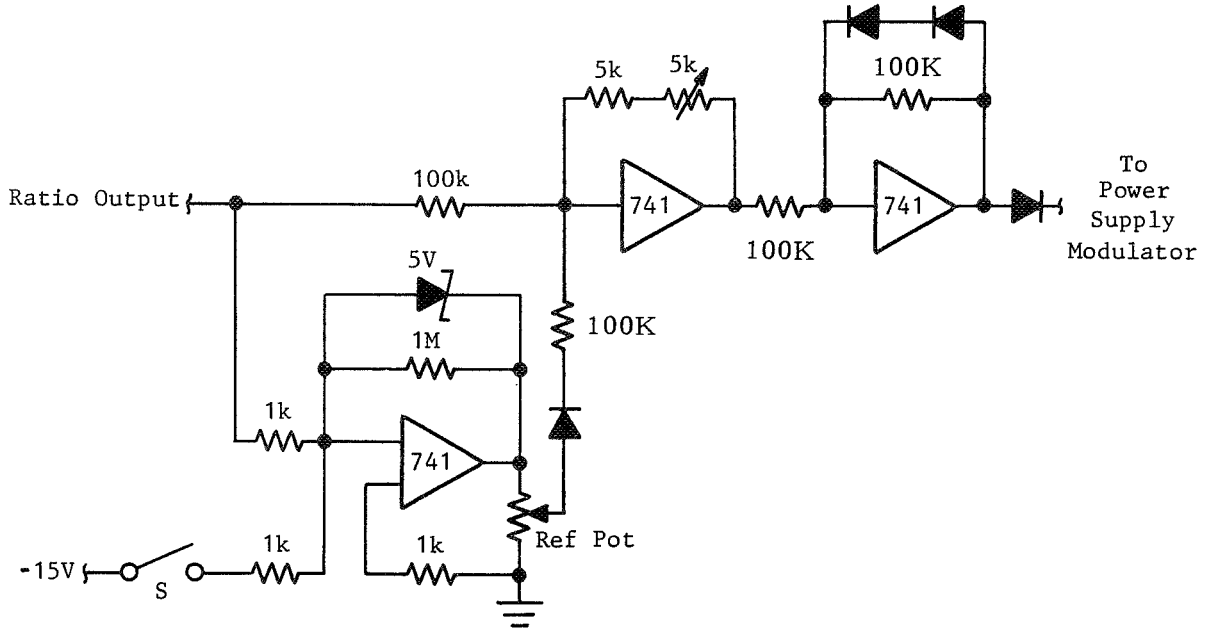


Figure 8. Control Electronics

The above device serves to provide a signal which is proportional to the difference between an adjustable reference and the output of the ratio unit.

Two problems were encountered in the controller worthy of note:

1 The adjustable reference had to be switched in and out at the proper times, since without switching the reference would Dc bias the controller and not provide the desired error signal. See Figure 9 for a graphical explanation which shows how these signals are time oriented.

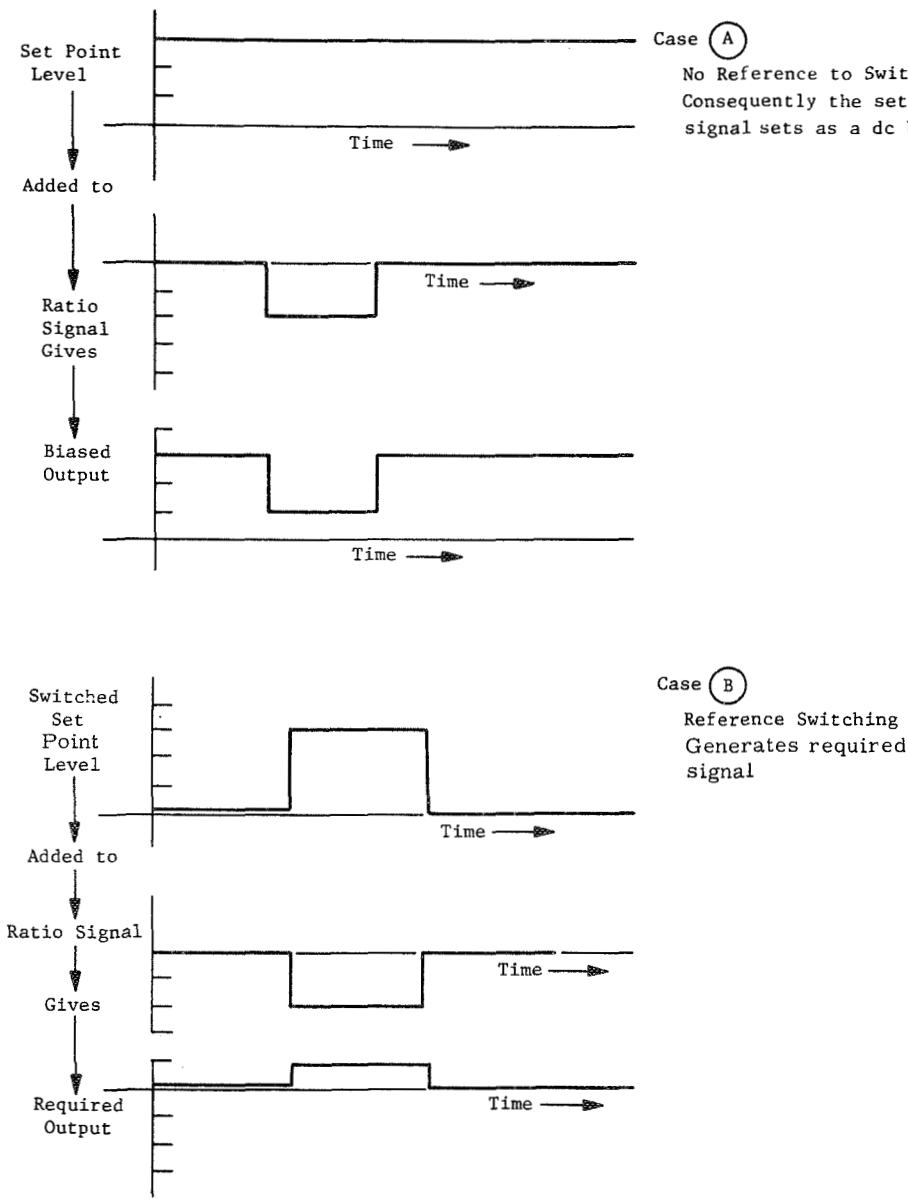


Case (B) gives the desired result.

Figure 9. Reference Switching

2 Because of the basic duty cycle oscillator, it was found that the relationship between controller output and duty cycle in the power supply was not a straight line function. (See Figure 10.) As a result several diodes were added to the last stage in the controller. It was felt that the diode nonlinearity would help. The linearity is better with the diodes (see Figure 10) but clearly more work is needed in this area.

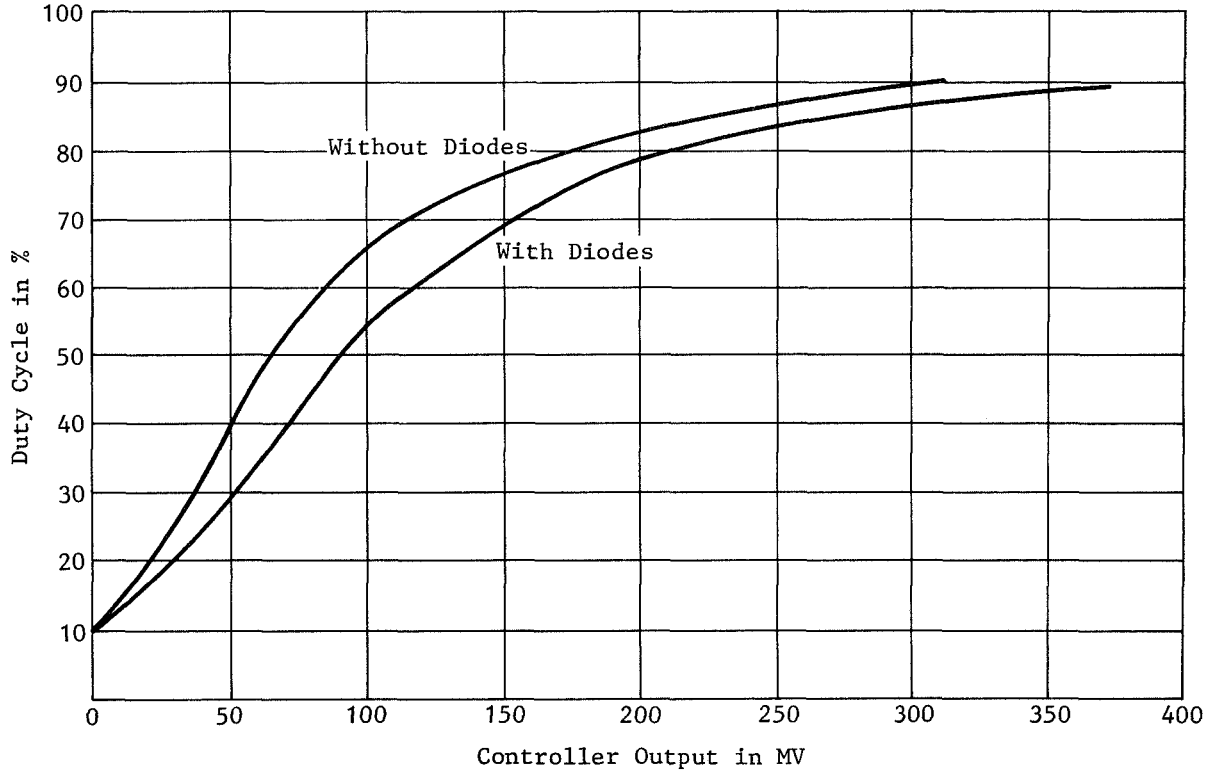


Figure 10. Controller Output With Duty Cycle

An overview of the breadboard controller is shown in Figure 12.

## C. POWER SUPPLY MODULATOR

Before total closed loop operation could be achieved, some method for modulating the energy available at the weld electrodes had to be devised. Of the several methods considered it was decided to switch the power supply capacitor bank in and out at a fixed frequency and to vary the duty cycle (in time versus out time) of that frequency. Figure 11 presents typical results, operating the power supply open loop.

The power supply monitor is shown in Figure 13. A detailed explanation of the working of the modulator and the modification necessary to the power supply is given in Appendix 3.

Channel 1 (Upper Trace) Vertical Scale - 0.1 Volt/CM
Channel 2 (Lower Trace) Vertical Scale - 1.0 Volt/CM

The upper trace is taken across a shunt in the secondary of the weld transformer. Photo No. 1 shows the chopped weld pulse with no error signal. The lower trace in Photos 2 and 3 is a simulated error signal demanding more or less energy at the weld joint as determined by the ratio of change in signal from the two IR sensors. Photo No. 4 shows the weld pulse modulated by a 100 Hz Sine wave error signal. The lower trace is the resultant duty cycle.

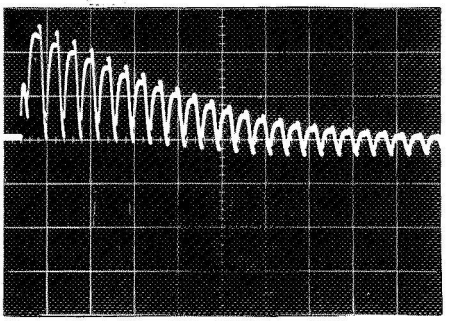

1. Time Base - 5 Msec/CM

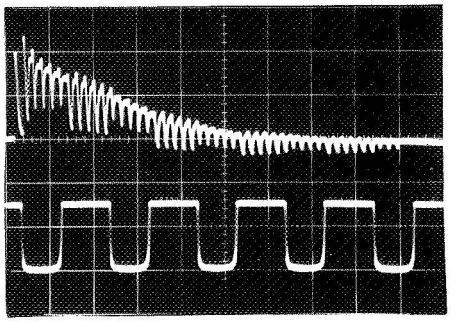

3. Time Base - 10 Msec/CM

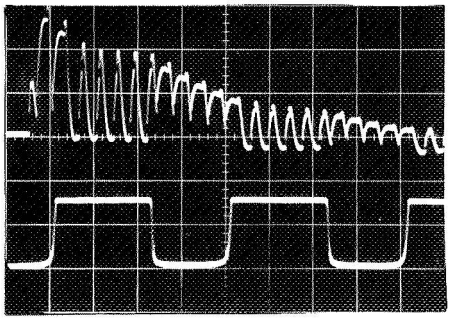

2. Time Base - 5 Msec/CM

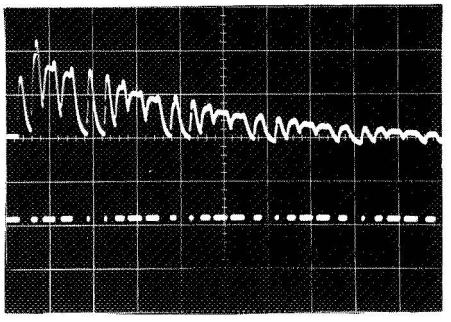

4. Time Base - 5 Msec/CM

Figure 11. Power Supply Operation

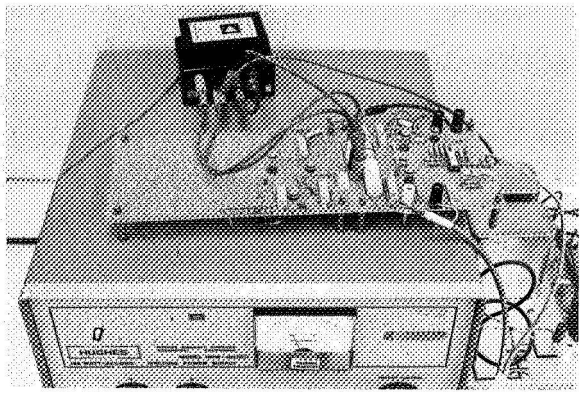

Figure 12. Breadboarded Controller

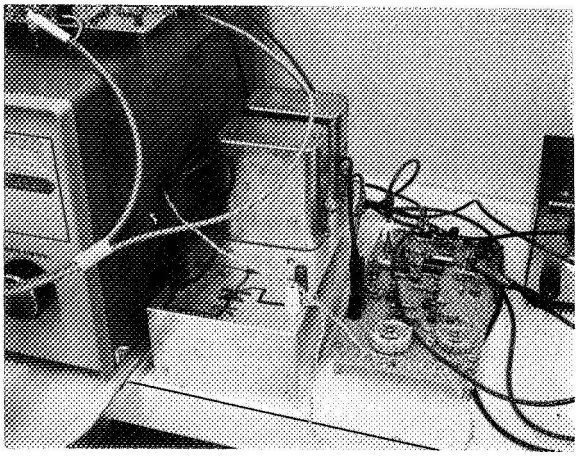

Figure 13. Breadboarded Modulator

## D. INVESTIGATION AND RESULTS

Once the control system had been developed, we could investigate the interplay between such parameters as modulation frequency, duty cycle, power supply watt/second setting and pull strength of the weld.

Considerable system data was taken, both open loop and closed loop.

Open loop data was taken by fixing the duty cycle and the modulation frequency and making welds at various power supply settings starting at 8 watt/seconds and continuing until expulsion occurred. The pull strength of these welds were recorded and plotted. Next the duty cycle was changed and the data taken again. Table I presents the points at which data was taken.

TABLE 1

Open Loop Data Points

| Frequency | Duty Cycle (Percent) | Watt - Seconds |
|---|---|---|
| 250 Hz | 10 | 8 → 24 |
| | 50 | 8 → 24 |
| | 90 | 8 → 24 |
| 500 Hz | 10 | 8 → 24 |
| | 50 | 8 → 24 |
| | 90 | 8 → 24 |
| 1 KHz | 10 | 8 → 24 |
| | 50 | 8 → 24 |
| | 90 | 8 → 24 |

The data set taken for a typical case (250 Hz) is presented in Figures 14, 15, 16. It should be noted that at this frequency (250 Hz) a 10 percent duty cycle produced a ratio which was a series of distinct pulses. It becomes open to question as to how to treat the data, although no adverse effects on the sample welds were observed. A condensation of the typical case plots is shown on Figure 17.

Closed loop data was taken by fixing the modulation frequency and zero control duty cycle. Welds were made at several power supply settings and various reference temperature settings. The pull strength of these welds were recorded and plotted. Typical case data is presented in Figure 18.

The closed loop behavior of the system was recorded on a storage oscilloscope and pictures taken. (See Figure 19).

In order to demonstrate the temperature variations with energy dissipated at the weld, the ratio unit output was recorded and photographed at 10, 15, 20 and 25 Ws setting on the power supply. Results of this experiment are given in Figure 20.

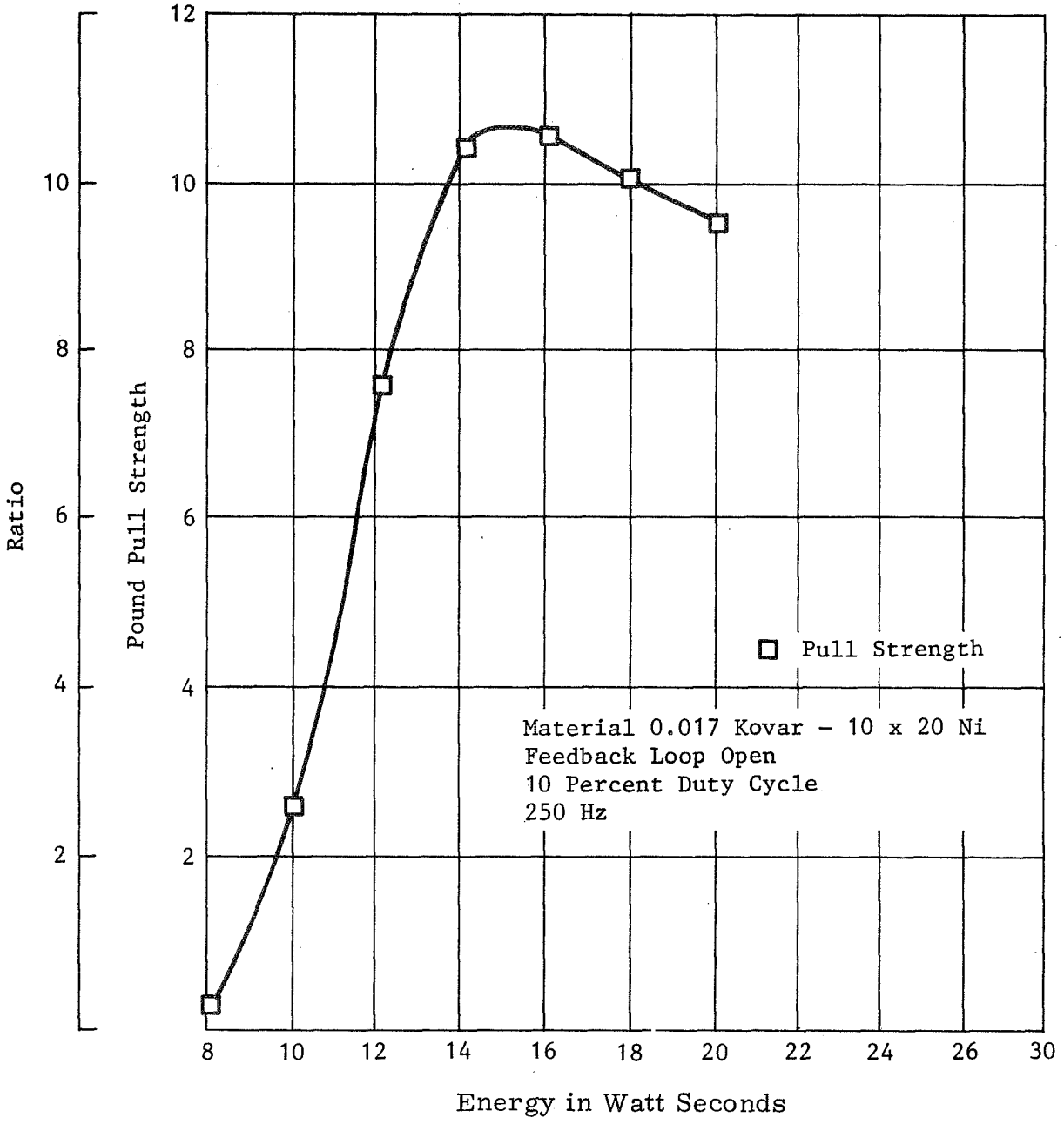


Figure 14. Open Loop Pull Strength Data

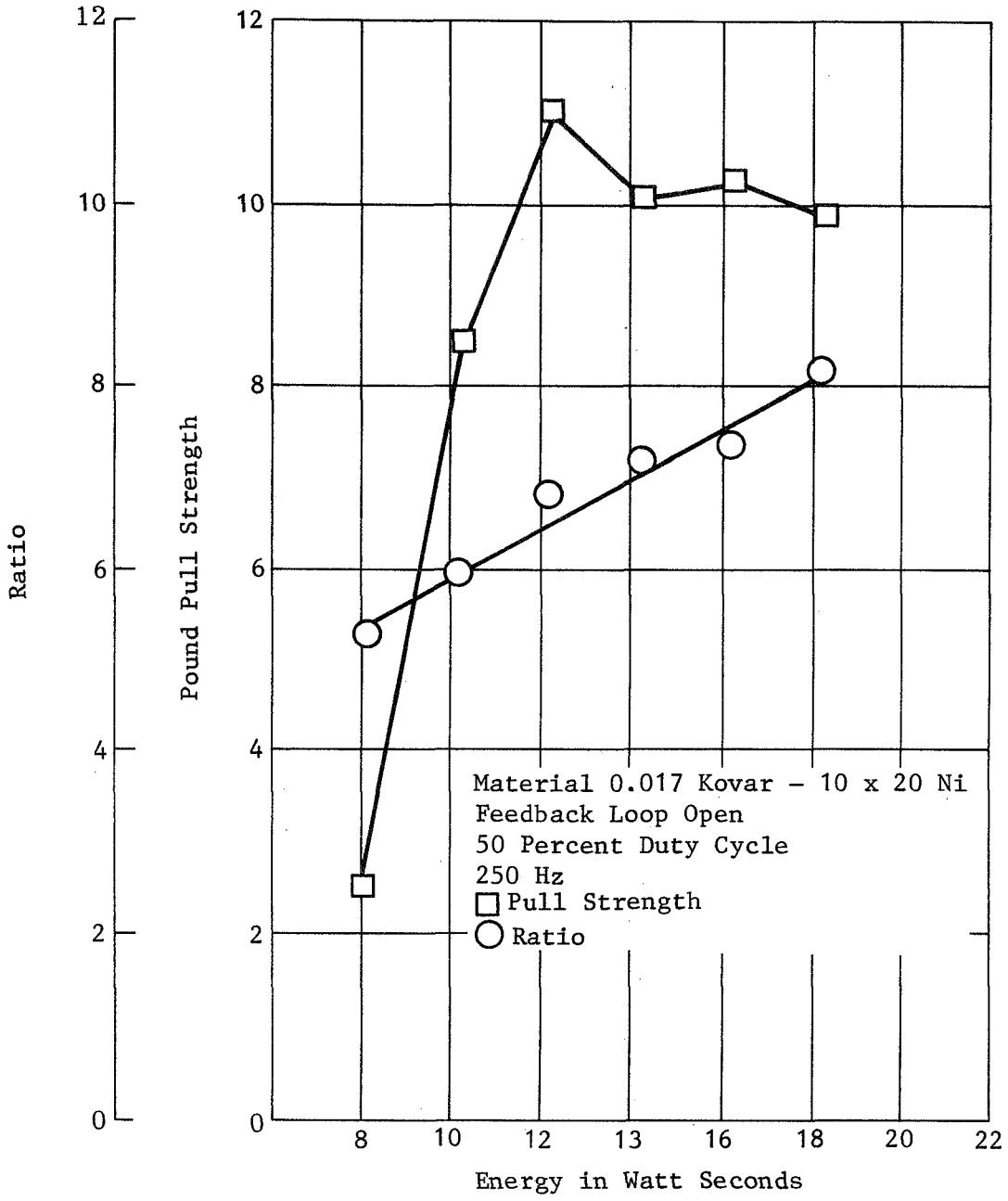


Figure 15. Open Loop Pull Strength Data

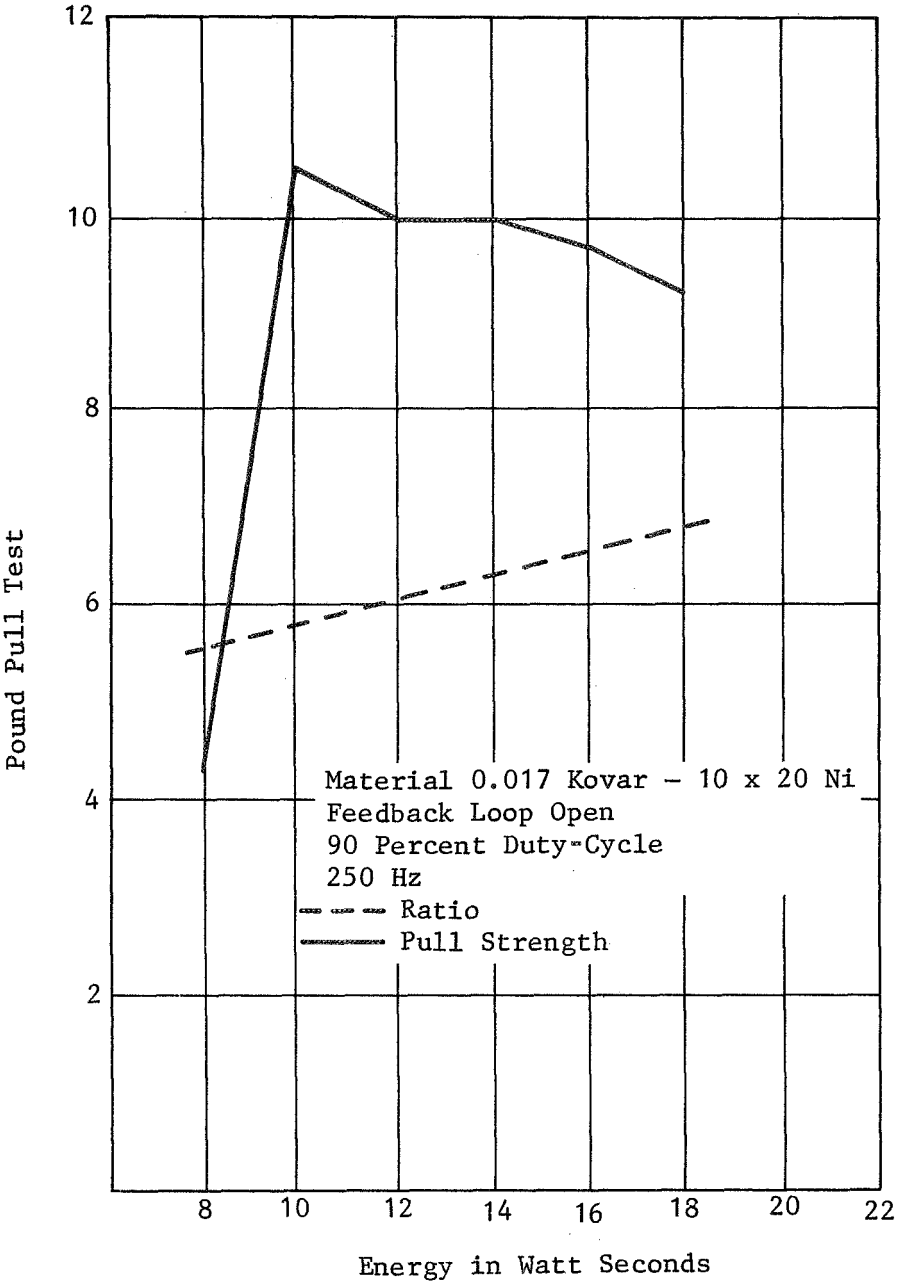


Figure 16. Open Loop Pull Strength Data

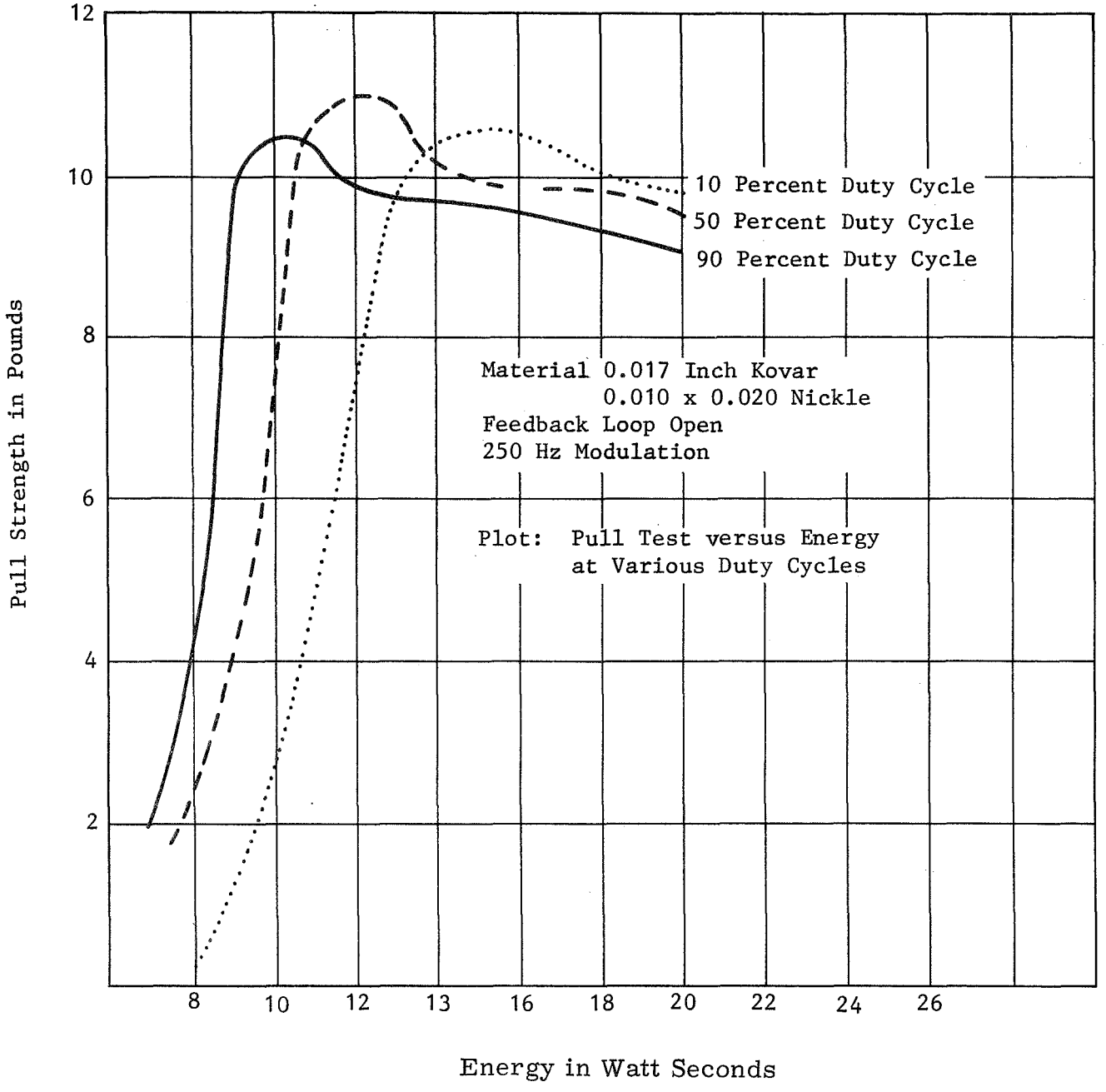


Figure 17. Summary Open Loop Data

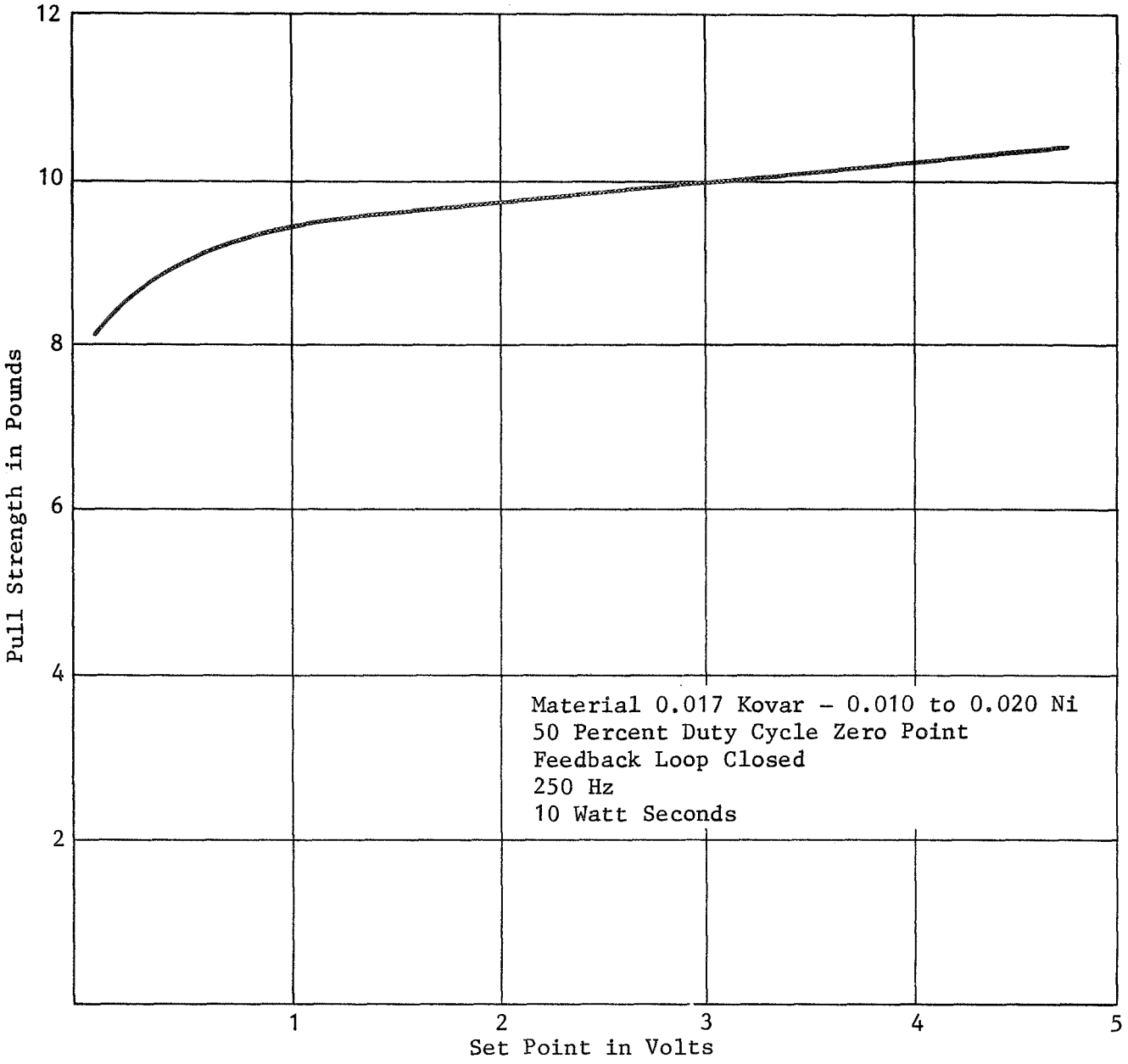


Figure 18. Closed Loop Data

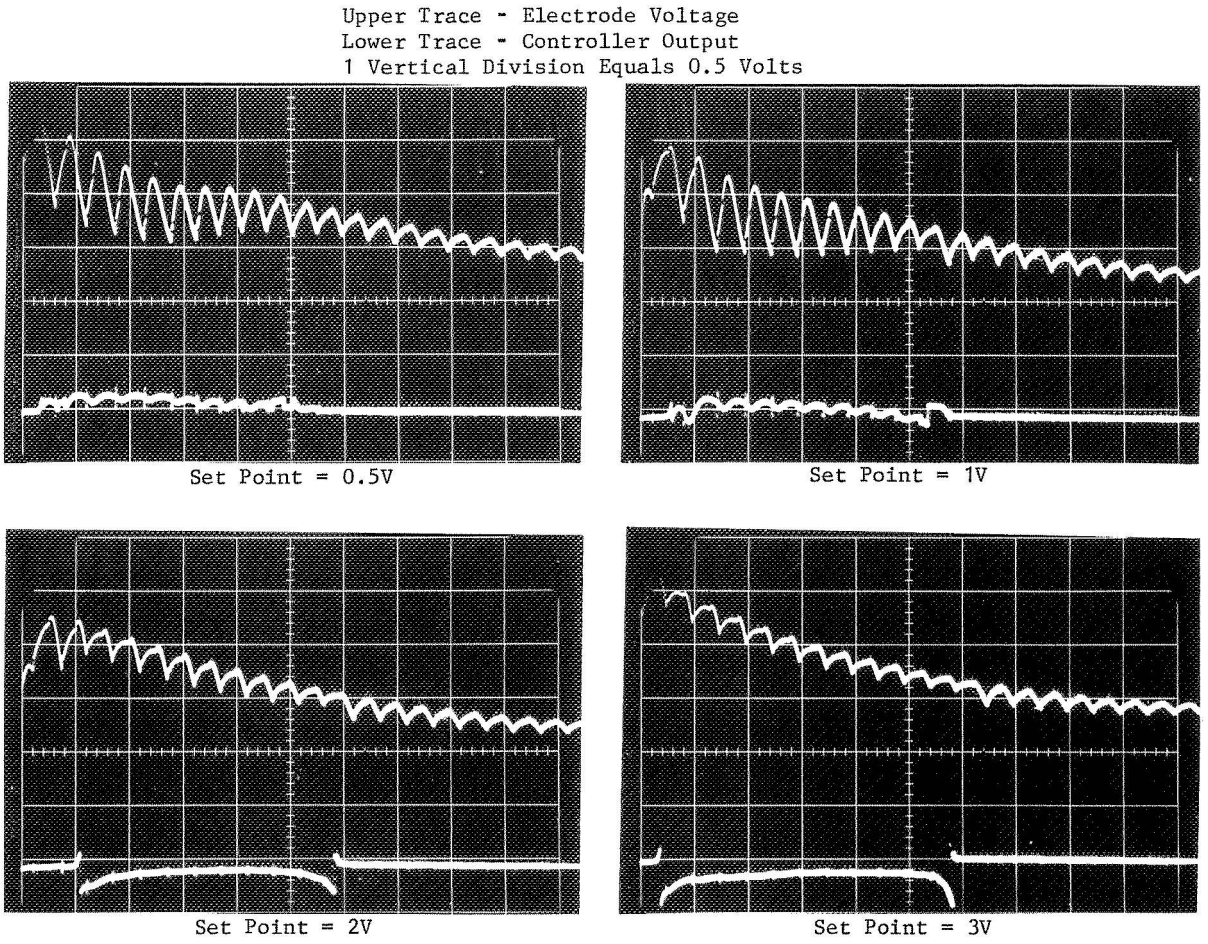


Figure 19. Closed Loop Behavior

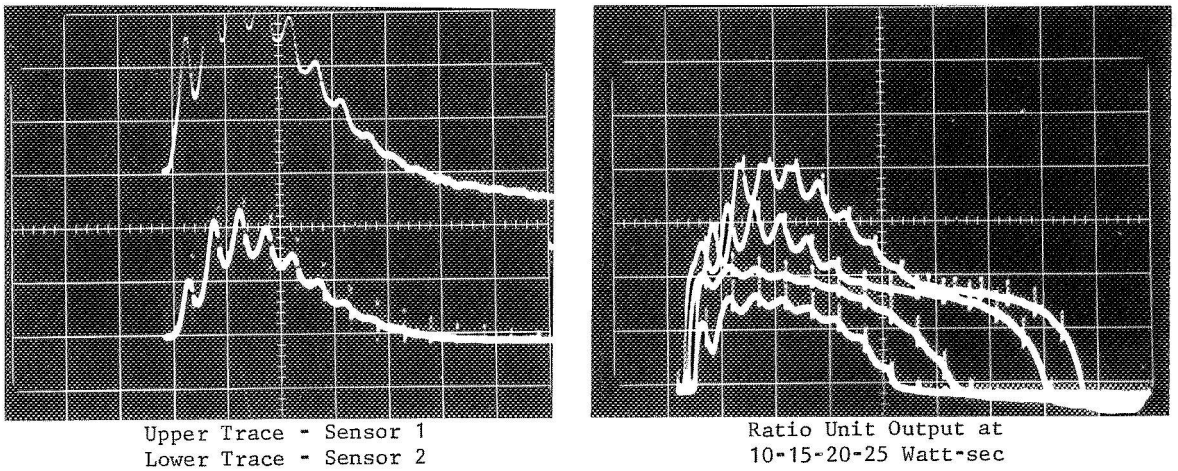


Figure 20. Ratio Unit Output

## E. DISCUSSION

The feasibility of monitoring the infrared radiation from a weld and using this information to effect closed loop control action has been clearly demonstrated. Further the concept of monitoring two discreet portions of the spectrum of radiated energy and inferring the actual temperature of the weld has also been proven feasible. The range of power supply settings in which it is possible to produce a satisfactory weld has been significantly extended using this technique.

As with any feasibility study, the end product is not a finished device. There are areas of concern and areas which have yet to be probed. Among these are:

1 The control action with set point should be improved. It is felt that several factors contribute to this state of affairs. The power supply is not a constant energy source. So that even with control, the initial part of the discharge may be sufficient to establish a weld. We have several ways out of this dilema. We can build temperature profiling into the system in an effort to impose severe restrictions on the power supply during the early portion of the weld cycle. Alternatively we can use control on the supply itself to make it a constant energy source. Under these conditions, it would make sense to use a standard pulse height and width and vary the rep-rate with the error signal.

2 Some sort of alignment aid whether mechanical, electrical or optical should be included in the sensor subsystem. A cone, the focal length of the lens, would seem to be the simplest solution. An alternative would be to use a fibre optics probe to minimize position errors. This would also alleviate electrical noise problems since cabling from sensor to controller would be eliminated. Fibre optics have the disadvantage that they cut-off energy transmission beyond 2.8 μm. However there should be sufficient energy in this region to effect a temperature measurement.

## F. RECOMMENDATIONS

As a result of the work performed under the present contract it is recommended that a production device, utilizing these techniques be designed and fabricated. Such an instrument could remove from the weld process:

1 Power supply variations

2 Component lead material variations

3 Pull strength variations

4 Error in operator judgement.

In addition, such a device could bring to the microweld process the reliability which is inherent in its nature.

## APPENDIX I

## DERIVATION OF DETECTOR EQUATIONS

Consider the basic circuit shown below.

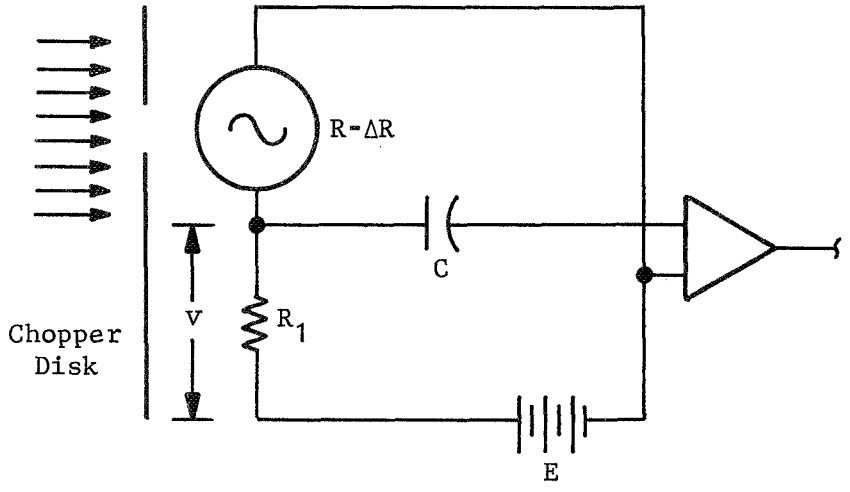


We assume that the IR device will change its resistance from R to R-ΔR when radiation impinges of the active area. So,

$$E = i(R + R_1)$$

$$V = i\,R_1 = \frac{R_1 E}{R + R_1}$$

$$-\frac{dV}{dR} = \frac{R_1 E}{(R + R_1)^2}$$

$$\Delta V = \frac{R_1 E\ \Delta R}{(R_1 + R_2)^2} = \frac{R_1}{R + R_1}\, i\ \Delta R = \beta i \Delta R \qquad (1)$$

where

$$\beta = \text{bridge factor} = \frac{R_1}{R + R_1}\,.$$

Now let the incident radiation be monochromatic and of frequency $\nu$.

Some definitions

h = Planck's constant

q = quantum efficiency = that fraction of the quanta incident on the detector that produce observable photo electric effects

n = number of effective quanta per area per unit time

w = power and corresponds to some constant source intensity.

Then,

$n = \frac{qw}{Ah\nu}$; A is the active area.

If N and P are the total number of electrons and holes in the detector element then R varies as $(bN + P)^{-1}$ where b is the mobility ratio. Since

$\Delta N = \Delta P$ in general,

$$\frac{dR}{dN} \simeq \frac{b + 1}{(bN + P)^2}$$

or

$$\Delta R \cong \frac{(b + 1)}{(bN + P)^2} \Delta N$$

$$\frac{\Delta R}{R} = \frac{(b + 1)}{(bN + P)} \Delta N \quad .$$

So,

$$\Delta V = \beta i \, \Delta R = \frac{Bi \, R(b + 1) \, \Delta N}{(bN + P)} \quad . \tag{2}$$

But $\Delta N$ is the change in the number of primary current carriers in the device. So we may say $\Delta N$ varies as I. The intensity or,

$$\Delta N = \gamma I \, (1 - e^{-t/\tau})$$

$$\therefore \Delta V = \left\{ \frac{\beta R(b + 1)}{(bN + P)} \right\} i\gamma \, I(1 - e^{-t/\tau}) \tag{3}$$

or,

$$\Delta V = \left\{ \frac{\beta R(b + 1)}{(bN + P)} \right\} \frac{qw\lambda}{h} \quad . \tag{4}$$

Equation (3) points out that the signal output from the detector ($\Delta V$) varies with source intensity. Equation (4) states that the output varies with $\lambda$, the wavelength.

If the radiation is not monochromatic, we have for total power:

$$w = \int_0^\infty w_\nu d\nu \quad .$$

So,

$$\Delta V = \frac{\beta R(b + 1)}{(bN + P)} \frac{1}{h} \int_0^\infty \frac{q(\nu)\ w_\nu d\nu}{\nu} \quad , \tag{5}$$

the above since $\lambda = \frac{1}{\nu}$ .

Now if we consider two such detectors with ideal narrow bandpass filters, and ratio their outputs, we get:

$$\frac{\Delta V_1}{\Delta V_2} = \frac{\dfrac{\beta R(b + 1)}{bN + P} \displaystyle\int_0^\infty \frac{q(\nu)\ w_{1\nu} d\nu}{\nu}}{\dfrac{\beta R(b + 1)}{bN + P} \displaystyle\int_0^\infty \frac{q(\nu)\ w_{2\nu} d\nu}{\nu}}$$

or,

$$\frac{\Delta V_1}{\Delta V_2} = \frac{w_1(\nu_1)}{w_2(\nu_2)} = K \quad . \tag{6}$$

In reality, these filters have finite bandpass. So,

$$w = \int_{\nu-\delta}^{\nu+\delta} w_\nu d\nu \quad .$$

And,

$$\frac{\Delta V_1}{\Delta V_2} = \frac{\int_{V_1-\delta}^{V_1+\delta} q(\nu_1)\, w_{\nu 1}\, \frac{d\nu_1}{\nu_1}}{\int_{V_2-\delta}^{V_2+\delta} q(\nu_2)\, w_{\nu 2}\, \frac{d\nu_2}{\nu_2}}$$

In the limit as $\delta \to 0$, the above reduces to Equation (6).

APPENDIX II

DERIVATION OF CIRCUIT EQUATIONS

A. Consider the following part of the sensor subsystem (See Figure 2).

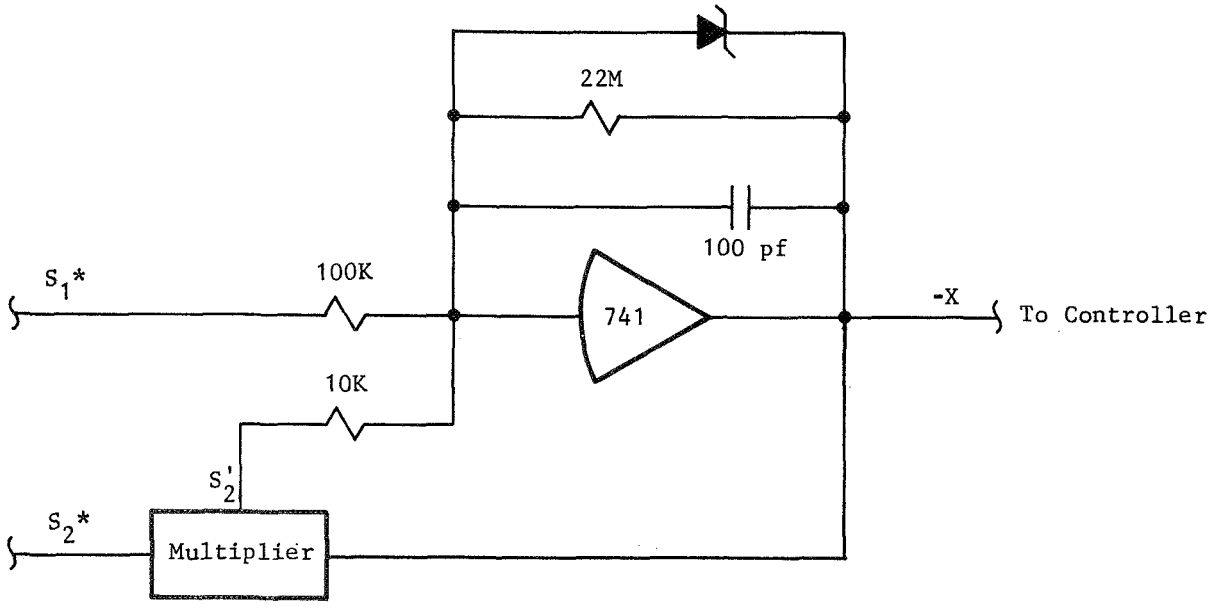


For the purpose of this discussion we can neglect the 22 meg resistor around the 741, since its only function is to provide a DC gain limit and very high frequency roll-off.

So

$$X = -\left(\frac{Z_f}{100K} S_1^* + \frac{Z_f}{10K} S_2'\right) \quad . \tag{1}$$

Where

$$Z_F \Big|_{X<10 \text{ volts}} = \frac{1}{CS} = \frac{1}{10^{-10} S} \quad .$$

Let

$$\tau_1 = 100 \times 10^3 \times 10^{-10} = 10^{-5}$$

$$\tau_2 = 10 \times 10^3 \times 10^{-10} = 10^{-6}$$

$S$ = Laplacian operator.

So

$$X = \left[\frac{1}{\tau_1 S} S_1^* + \frac{1}{\tau_2 S} S_2'\right] . \tag{2}$$

But

$$S_2' = \frac{XS_2^*}{10} .$$

So

$$X = -\left[\frac{1}{\tau_1 S} S_1^* + \frac{1}{\tau_1 S} X S_2^*\right] . \tag{3}$$

And

$$X + \frac{X S_2^*}{\tau_1 S} = \frac{1}{\tau_1 S} S_1^*$$

$$\therefore X = -\frac{S_1^*}{S_2^*}\left[\frac{1}{\frac{\tau_1}{S_2^*} S+1}\right] = \text{Ratio} \tag{4}$$

With $S_1^* = S_2^*$ = unity the corner frequency should be about

$$w = \frac{1}{\tau} = \frac{1}{10^{-5}}$$

$$f = 0.157 \times 10^5 = 15.7 \text{ KHz.}$$

However the 741 will roll off prior to that point.

B. Detector Impedance matching amplifier.

Consider the following:

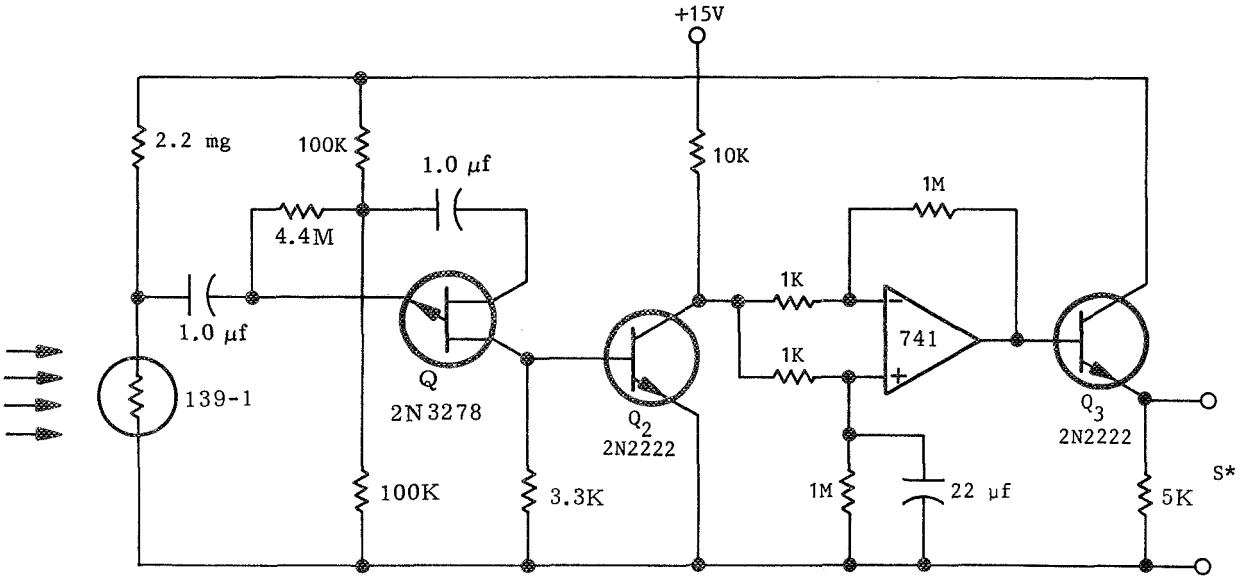


The 2N3278 is a p-channel junction FET used as a source follower. The junction FET and transistor $Q_2$ used in cascade have an overall gain of slightly less than one.

The circuitry around the 741 behaves as follows, consider the generalized case

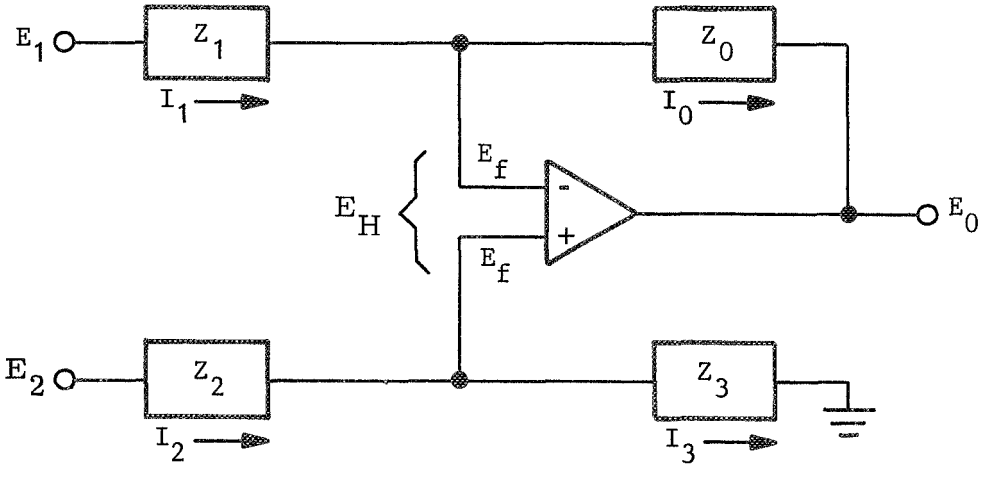

Now ideally

$$I_o = I_1$$

$$I_2 = I_3$$

$$E_H = 0 \quad .$$

So

$$E_f = \frac{Z_3}{Z_2 + Z_3} E_2 \tag{5}$$

$$I_1 = \frac{E_1 - E_f}{Z_1} = \frac{E_f - E_o}{Z_o} \tag{6}$$

$$-E_o = \frac{Z_o}{Z_1}(E_1 - E_f) - E_f \tag{7}$$

$$-E_o = \frac{Z_o}{Z_1} E_1 - \frac{Z_0}{Z_1} Ef - \frac{Z_1}{Z_1} Ef. \tag{8}$$

Or

$$E_0 = \frac{Z_o}{Z_1} E_1 + \frac{Z_o + Z_1}{Z_1} Ef. \tag{9}$$

Substitute for $E_f$

$$E_o = \frac{Z_o + Z_1}{Z_1} \left( \frac{Z_3}{Z_2 + Z_3} \right) E_2 - \frac{Z_o}{Z_1} E_1 \quad . \tag{10}$$

But

$$Z_o = 1M$$

$$Z_1 = 1K$$

$$Z_2 = 1K$$

$$Z_3 = \frac{1M}{22\ S+1}$$

$$E_2 = E_1 \quad .$$

So

$$E_o = \left(\frac{1M+1K}{1K}\right)\left(\frac{\frac{1M}{22\ S+1}}{1K+\frac{1M}{22\ S+1}}\right)E_1 - \frac{1M}{1K}E_1.$$

Or

$$E_o = \left\{\left(\frac{1M+1K}{1K}\right)\left(\frac{1M}{1M+1K\ (22\ S+1)}\right) - \left(\frac{1M}{1K}\right)\right\}E_1 \qquad (11)$$

at DC

$$\underset{S\to o}{\text{LIMIT}}\ E_o = \left(\frac{1M}{1K} - \frac{1M}{1K}\right)E_1 = o.$$

At high frequency

$$\underset{S\to\infty}{\text{LIMIT}}\ E_o = -\frac{1M}{1K}E_1 = -1000\ E_1.$$

Simplifying equation (11) we get

$$E_o = \frac{-22S}{0.022\ S+1}$$

Frequency response is given below

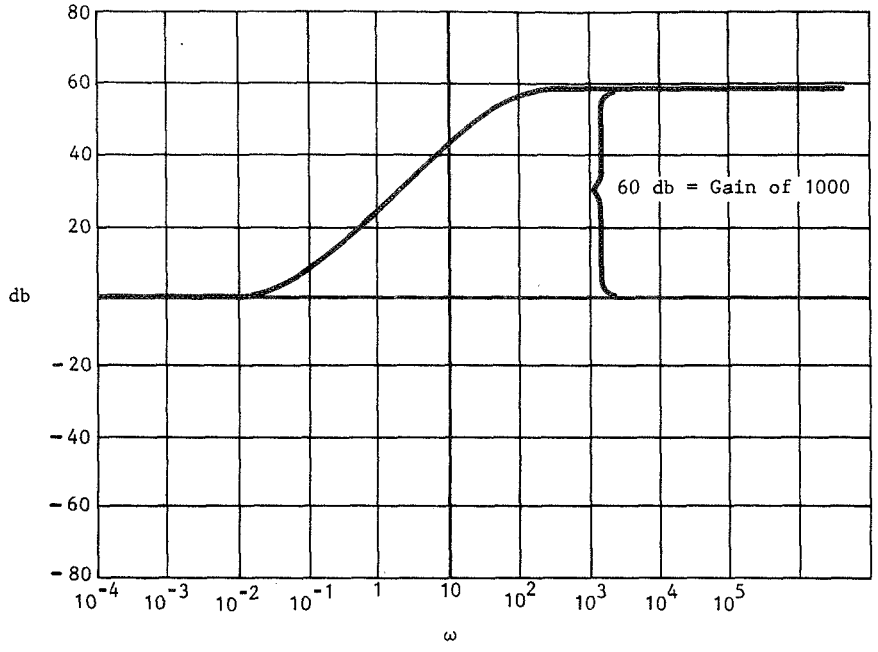

## APPENDIX III

## A. SOLID STATE WELD POWER SUPPLY

### DESCRIPTION AND MODIFICATIONS

The weld power supply (See Figures 1 and 2 this appendix) consists of two major assemblies; the power section and the control section. The power section is made up of a charge level selecter which is essentially a variable transformer driven by a step up transformer. This is connected to the 115VAC line. A rectifier unit which is made up of a full wave bridge rectifier and series SCR which is normally in a conducting state, and the energy storage unit with the associated circuits to discharge the energy to the weld transformer upon receipt of a trigger signal from the control circuitry.

The control section is made up of three time delays and the trigger circuit for SCR 2. The time delays are started by a weld signal from the operators foot switch. The first time delay determines the weld repetition rate and is of sufficient length to allow complete discharge and recharge of the energy storage bank before a second weld can be attempted. The second delay prevents recharge of the energy bank until it is completely discharged. This is accomplished by removing the gate signal from the SCR in the rectifierfier and series control unit (SCR1). The third timer delays the trigger to SCR2 for a minimum time base of one-half cycle of line frequency. This is in order to ensure that SCR1 has ceased to conduct before SCR2 is gated into conduction.

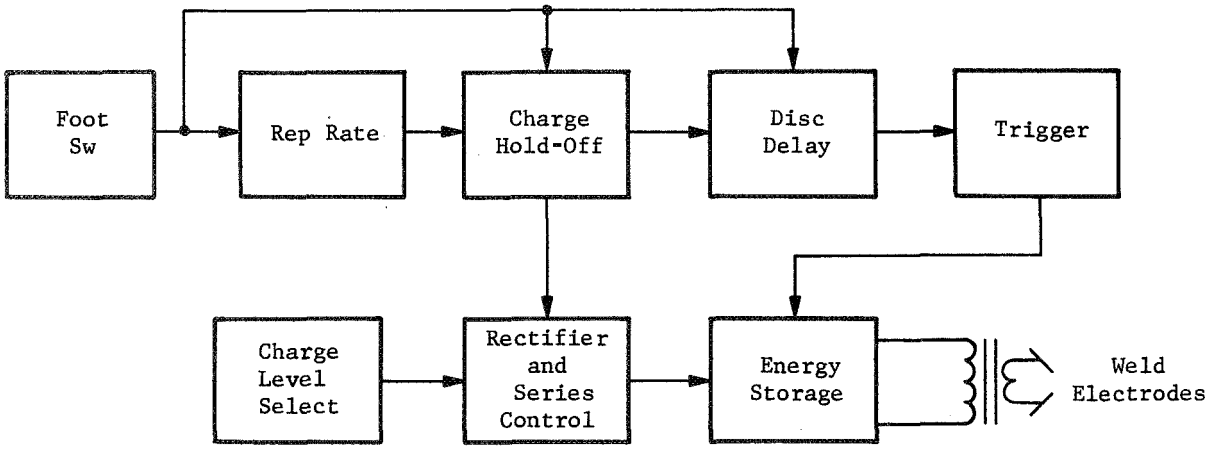


Figure 1. Block Diagram Weld Supply

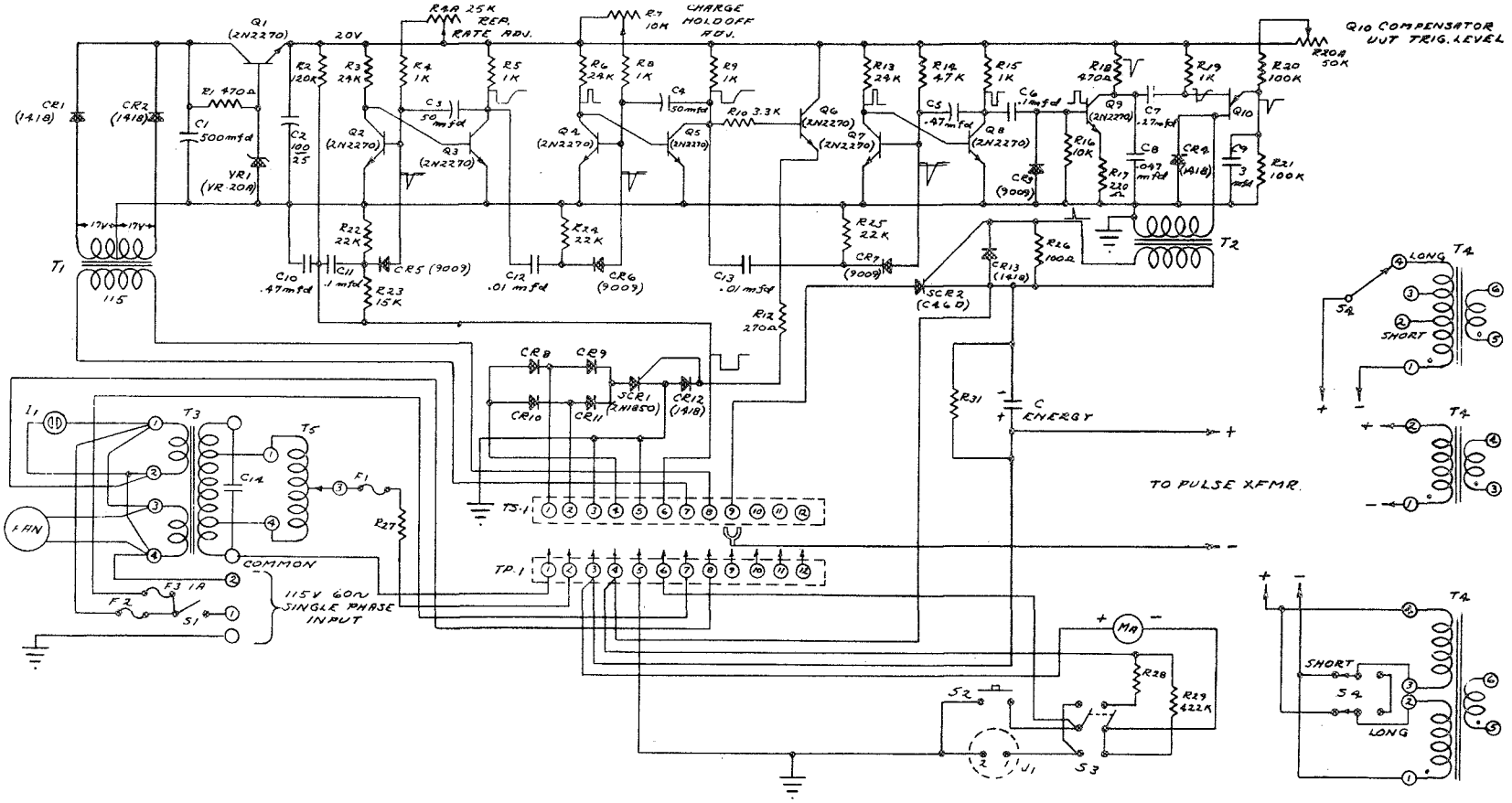


Figure 2. Schematic Weld Supply

The first two time delays are adjustable but it was necessary to increase the times beyond their range by doubling the size of the timing capacitors (C3 and C4). This was necessary because we have purposely lengthened the weld current pulse in order to exercise better control. The third time delay is fixed and no change in it was necessary.

The other modifications to the weld power supply included insertion of resistance in the anode of SCR2. Its existing trigger circuit was disconnected. SCR2 is now driven by the outboard control circuitry.

## B. FEEDBACK TRIGGER AND MODULATOR

The basic operation of the modulator is as follows:

Q101 (See Figure 3 this appendix) is a free running oscillator, the frequency of which is adjustable from 150 Hz to 2K Hz. Pulses developed across the base 1 resistor are coupled to signal conditioning transistor Q102. These pulses appear at the collector as fast going square waves and are directly coupled to IC1, a JK Flip-Flop. Without the inhibit signal at pin 13 the flip-flop would operate as a ripple counter producing alternate square waves at the two outputs, the pulse rate at either output being one-half the frequency of Q101. This action is prevented, however, by the grounded input at pin 12 and under quiescent conditions pin 4 of the FF is in a low state and pin 9 is high. These signals are inverted by amplifiers Q103 and Q104 and emitter follower Q110 prevents current flow to Q111.

Q113 and Q114 make up a conventional monostable multivibrator, or one shot, the time base of which is adjustable by R102. The oneshot is triggered by a negative going signal from the weld power supply. The output is inverted by Q115 which in turn controls the action of the flip-flop.

Q112 is a keyed oscillator that is adjusted by R105 to operate at a frequency twice that of Q101 for a 50 percent weld duty cycle. It is only allowed to operate when current is supplied by Q110 and Q111 to the charge capacitor connected to the emitter. This capacitor is initially charged to a level slightly below the firing potential of Q112 by voltage divider R103 and R104. This assures that the time duration between pulses developed across the Base 1 resistor are not effected by base two to emitter leakage of Q112. The output signal from this oscillator is also fed to the input of the flip-flop. Q111 acts as a variable resistor in series with the charge capacitor. This resistance varies with the error signal from the controller.

When the operator initiates a weld signal a negative going pulse is generated by Q9 in the weld power supply. This signal triggers the one shot made up of Q113 and Q114. This allows the flip flop to operate throughout the time duration of the one shot. When the flip flop changes states SCR2 in the weld power supply fires as a result of a signal through Q104, Q107 and Q108. The conduction of SCR2 allows current to flow in the primary of the weld transformer and C1 charges to the level of the energy bank. This charge is held by the reverse diodes across SCR 101. At the time the flip flop changed states, Q104 drives Q110 into conduction and current is supplied to the charge

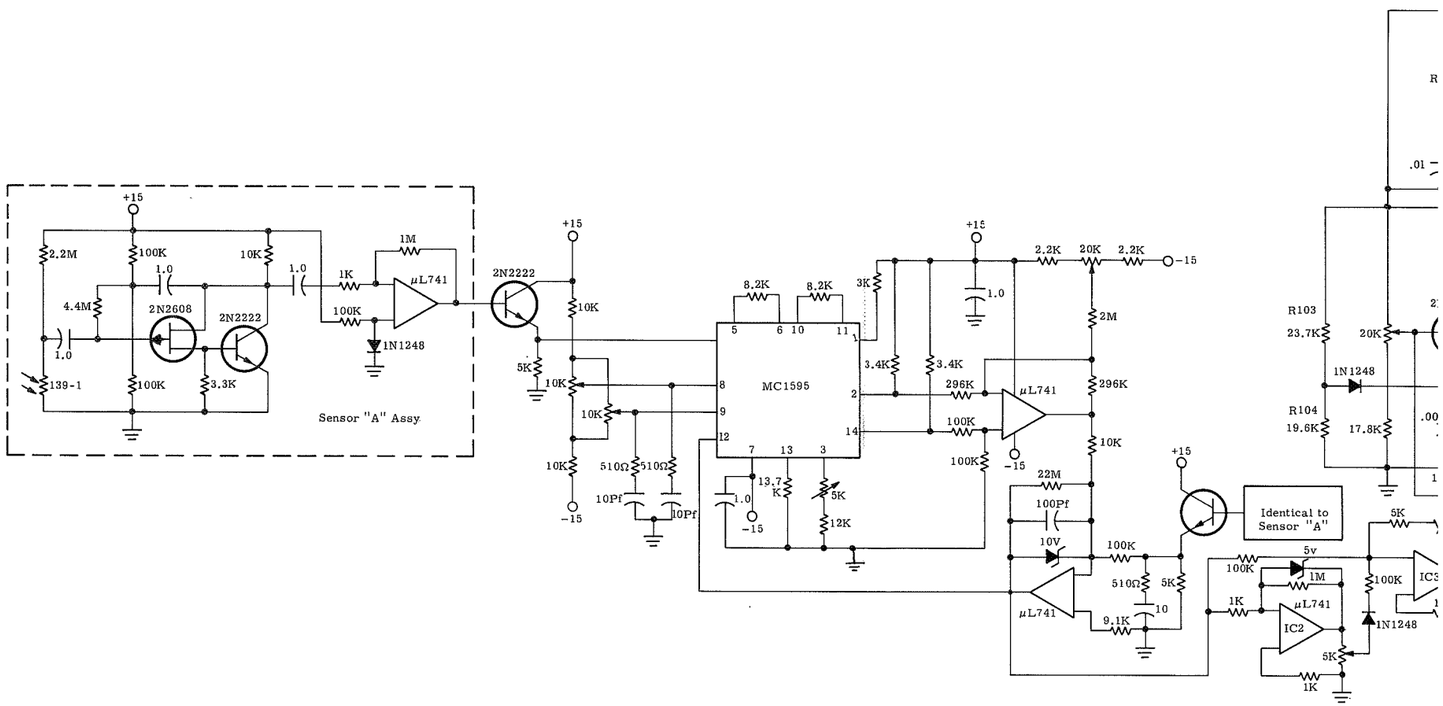


All Capacitors in Microfarads
Except as Otherwise Noted

| Symbol | HRW-50 | HRW-100 | HRW-250 |
|---|---|---|---|
| C-Energy | 600mfd | 1200mfd | 3000mfd |
| R27 | 6 ohm | 6 ohm | 1 ohm |
| R31 | 20K | 20K | 10K |
| R28 | 374K | 374K | 332K |
| F1 | 2A S.BLO | 3A S. BLO | 5A S. BLO |
| F2 | 3A S.BLO | 5A C. B. | 8A C.B. |
| F3 | | 1 AMP 3 AG | |

Figure 3. Complete System

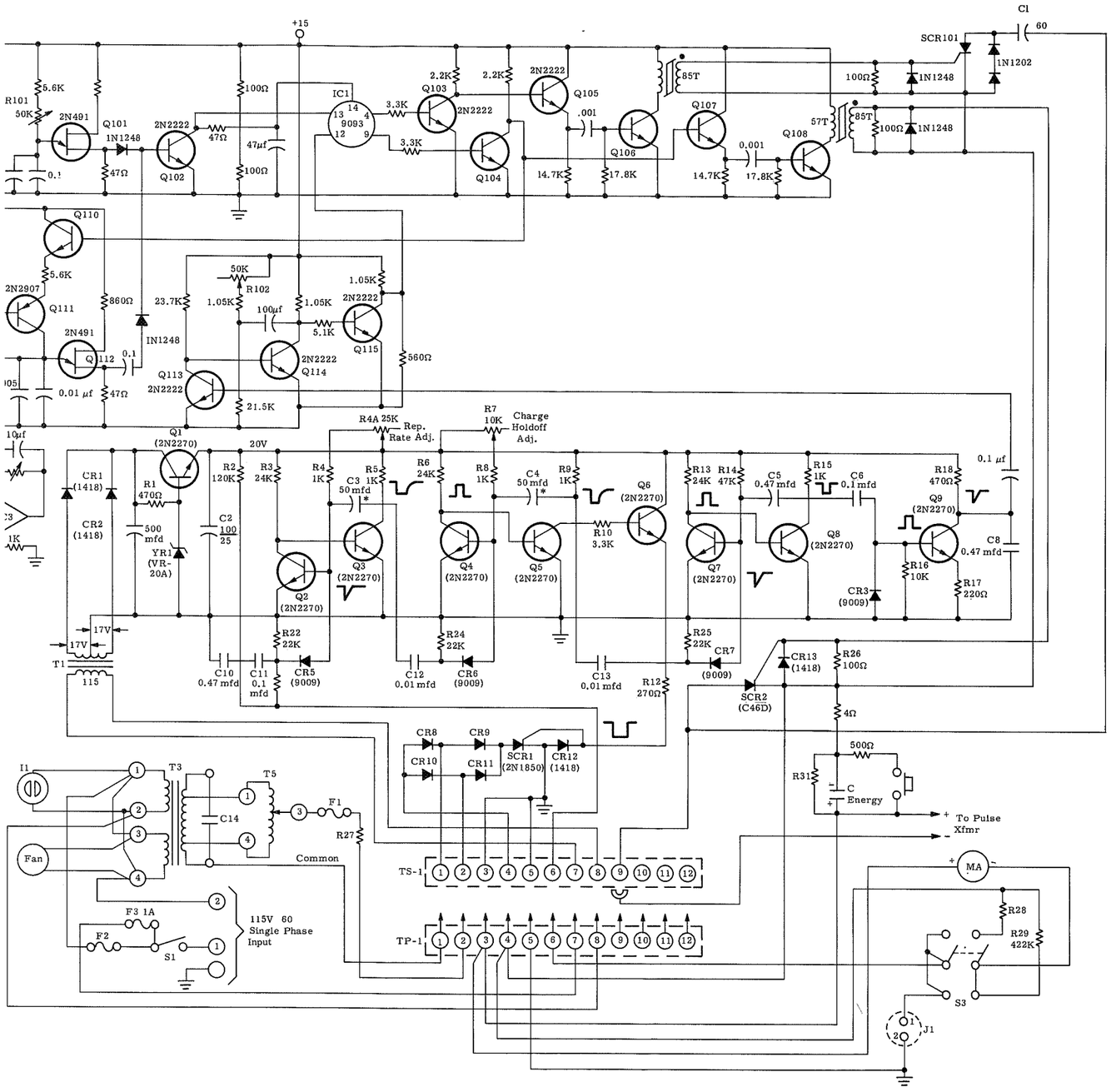
+15
C1
60
SCR101
1N1202
1N1248
100Ω
85T
57T
R101
50K
5.6K
2N491
Q101
1N1248
2N2222
47Ω
Q102
47μf
100Ω
0.1
IC1
9093
3.3K
Q103
2.2K
2N2222
Q104
Q105
.001
Q106
14.7K
17.8K
Q107
Q108
0.001
Q110
2N2907
Q111
860Ω
IN1248
2N491
Q112
0.01 μf
47Ω
50K
R102
23.7K
1.05K
100μf
5.1K
2N2222
Q115
Q113
2N2222
Q114
560Ω
21.5K
R4A 25K
Rep. Rate Adj.
R7
10K
Charge Holdoff Adj.
Q1
(2N2270)
20V
CR1
(1418)
CR2
(1418)
R1
470Ω
500 mfd
YR1
(VR-20A)
R2
120K
C2
100
25
R3
24K
R4
1K
R5
1K
C3
50 mfd
R6
24K
R8
1K
C4
50 mfd
R9
1K
Q6
(2N2270)
R10
3.3K
R13
24K
R14
47K
C5
0.47 mfd
R15
1K
C6
0.1 mfd
R18
470Ω
0.1 μf
Q9
(2N2270)
C8
0.47 mfd
R16
10K
R17
220Ω
CR3
(9009)
Q2
(2N2270)
Q3
(2N2270)
Q4
(2N2270)
Q5
(2N2270)
Q7
(2N2270)
Q8
(2N2270)
17V
17V
T1
115
R22
22K
C10
0.47 mfd
C11
0.1 mfd
CR5
(9009)
R24
22K
C12
0.01 mfd
CR6
(9009)
C13
0.01 mfd
R25
22K
CR7
(9009)
R12
270Ω
SCR2
(C46D)
CR13
(1418)
R26
100Ω
4Ω
CR8
CR9
CR10
CR11
SCR1
(2N1850)
CR12
(1418)
500Ω
R31
C
Energy
To Pulse Xfmr
I1
T3
T5
C14
F1
R27
Fan
Common
TS-1
TP-1
MA
R28
R29
422K
S3
J1
F3 1A
F2
S1
115V 60
Single Phase
Input

capacitor at the emitter of Q112 via the series transistor Q111. Transistor Q112 fires at some later time determined by the signal at the base of Q111. The firing of Q112 causes the flip flop to revert to its original state and SCR 101 is gated into conduction as a result of the signal through Q103, Q105 and Q106. The conduction of SCR 101 reverse biases SCR2 in the weld power supply and it switches to a non conducting state. SCR 101 ceases to conduct when the charge on C1 is depleted. This process continues for a time determined by the time base of Q113 and Q114, with Q101 turning the weld supply on at a fixed rate and Q112 turning it off at a time determined by the time constant of Q111 and the charge capacitor. Since the resistance of Q111 is varied by the signal at its base the duty cycle of the weld power supply may be varied from 10 to 90 percent by the error signal.

## REFERENCES


1. ''Study on Development of Techniques for Resistance Welding.'' Final Report Contract No. NAS8-20339

2. ''Design Manufacture and Test of Infra-Red Cross Wire Resistance Micro-Welding System.'' Final Report Contract No. NAS8-21221

3. ''Infrared Preweld and Weld Monitor'', Martin Marietta Corp. Internal Report William G. Cunningham, December 1969

4. ''The Detection and Measurement of Infra-Red Radiation.'' Smith, Jones and Chasmar. Second Edition

5. ''An Introduction to the Principles of Infra-Red Physics.'' Hayes International Corporation. Fourth Edition